Journal of Luminescence xxx (xxxx) 121963

Contents lists available at ScienceDirect

Journal of Luminescence

journal homepage: www.elsevier.com/locate/jlumin

Full Length Article

Photochromic and fluorescence switching behavior of triazole-functionalized fulgimides: Experimental and theoretical study

Khamis Nassor Ally[a,*], Melkizedeck Hiiti Tsere[a], Said Ali Vuai[a], Azaria Stephano Lameck[b], Leyla Öztürk[c], Mahmut Köse[c]

[a] Department of Natural Science, College of Science and Technical Education, Mbeya University of Science and Technology, PO Box 131, Mbeya, Tanzania
[b] Department of Earth Science, College of Science and Technical Education, Mbeya University of Science and Technology, PO Box 131, Mbeya, Tanzania
[c] Department of Chemistry, Faculty of Science, Zonguldak Bülent Ecevit University, Zonguldak, Turkey

ARTICLE INFO

Keywords:
Photochromism
Fulgide
Fulgimide
Triazole
Fluorescence switch

ABSTRACT

Integrating photochromism and fluorescence switching within a single molecular platform remains a central challenge in the development of light-regulated functional materials. Here, we report a structure-encoded design strategy based on the direct covalent incorporation of a 1,2,4-triazole unit into the imide framework of fulgimides, yielding three new photoresponsive molecules (**4E–6E**). Experimentally, all compounds exhibit photochromism based on the interconversion between open and closed forms. This is accompanied by large visible-range spectral contrast and reversible fluorescence ON/OFF switching under alternating UV and visible light.The open-ring forms are strongly emissive, while photoinduced cyclization produces systematic fluorescence quenching (20–40%) governed by intramolecular energy transfer to the conjugated closed-ring core. Density functional and time-dependent DFT calculations quantitatively reproduce the observed experimental absorption behavior and reveal pronounced π-delocalization and HOMO-LUMO gap narrowing upon ring closure, establishing clear structure–property relationships. Among the series, compound **6E** shows the most favorable electronic and optical characteristics. These results identify triazole-imide coupling as a generalizable molecular engineering route for multifunctional organic photo-switches and advance their potential for optical memory, sensing, and adaptive photonic applications.

1. Introduction

Photochromic compounds that undergo reversible isomerization under light irradiation have attracted extensive interest for applications in molecular electronics, optical data storage, and dynamic sensing [1–6]. Among them, fulgimides combine exceptional thermal stability with irreversible 6π-electrocyclization behavior, distinguishing them from other photochromic scaffolds. Integrating fluorescence functionality into such systems remains a formidable challenge, as it requires precise control of excited-state dynamics to achieve reversible on/off emission switching [6–8]. Additionally, they exhibit superior photochromic performance, and increased resistance to hydrolysis [9,10]. Furthermore, the nitrogen atom in their imide group allows for versatile structural modifications. While many photochromic fulgimides have been synthesized and studied for their thermal stability and fatigue resistance [11,12], very few have been reported that can also switch fluorescence on and off.

A key challenge in materials science is synthesizing molecules whose fluorescence can be precisely turned on and off using light [13–15]. Typically, this involves a photochromic system where one molecular state (for example, the "open" form) fluoresces brightly, while its alternate state (the "closed" form) does not. In most photochromic systems, only one form of the molecule (e.g., the open form) is fluorescent, while the other (e.g., the closed form) is nonfluorescent [16]. By using specific wavelengths of light to switch the molecule back and forth between these two states, scientists can effectively control its light emission. This reversible control is highly valuable for industrial applications, including optical data storage, bioimaging, and molecular-scale switches [11,17–19]. Sivasankaran and Palaninathan developed a photoswitchable fluorescent film by electropolymerizing a special pyrrole monomer on an ITO electrode. They reported that the resulting polypyrrole film, which contained 2-indolylfulgimide, could switch its fluorescence on and off [20]. When the fulgimide was in its open form, the polypyrrole emitted visible light between 500 and 600 nm. However, when the

* Corresponding author.
E-mail address: khamisnassor2016@gmail.com (K.N. Ally).

https://doi.org/10.1016/j.jlumin.2026.121963
Received 27 March 2026; Received in revised form 10 May 2026; Accepted 11 May 2026
0022-2313/

fulgimide switched to its closed form, the fluorescence quenched. The authors attribute this quenching to Förster resonance energy transfer (FRET) from the polypyrrole to the closed-form fulgimide [20,21].

Photochromic molecules that exhibit fluorescence modulation function as molecular-scale fluorescent switches since their fluorescence can be turned on and off as their structure changes with light. This property makes them highly useful for super-resolution fluorescence microscopy [22–26]. Compounds with a triazole ring are of great interest because they often possess a wide range of valuable biological properties, including antiviral, antibacterial, and anti-HIV activities [27–29]. Beyond biology, these triazole-containing compounds are also useful in industrial applications as dyes, corrosion inhibitors, sensors, and photostabilizers [30,31]. Additionally, photochromic-fluorescent triazole-linked 2-indolylfulgimide polymers were synthesized by Nithyanandan et al. [32], which demonstrated fluorescence modulation in fulgimide-based and triazole-containing systems; however, these systems typically suffer from limited thermal stability or incomplete fluorescence reversibility. Interestingly, both the open-form and the closed-form of this triazole-fulgimide displayed fluorescent properties. The studied triazole-fulgimide polymer is considered to have potential application in optical memory and optical switching systems [33–35].

Recent work has shown that embedding triazole-based fluorophores within photochromic diarylethenes enables efficient, light-controlled fluorescence switching. Ding and co-workers demonstrated that a triazole-quinoline-bridged diarylethene exhibits reversible fluorescence on/off switching upon photoinduced ring opening and closure [36]. Coordination with Zn^{2+} generates a strong emission, which is efficiently quenched in the closed form through Förster resonance energy transfer to the conjugated diarylethene core. These findings established triazole-functionalized diarylethenes as viable platforms for fluorescence switching and chemical sensing [1,36,37]. Despite advances in photochromic-fluorescent integration, the underlying structure-property correlations governing triazole-induced electronic modulation in fulgimides remain poorly understood. Notably, no photochromic fulgimide has been reported in which a triazole unit is directly and covalently integrated into the imide functionality, leaving a critical gap in structure-property understanding at the interface of triazole chemistry and fulgimide photochromism. To address this challenge, we report the synthesis of a new class of 1,2,4-triazole-linked fulgimide photochromes and present a comprehensive investigation of their photochromic and fluorescence properties in solution. In parallel, detailed theoretical studies based on density functional theory (DFT) and time-dependent DFT (TD-DFT) were performed to probe the geometrical and electronic factors influencing their photochromic behavior. The integration of experimental results with computational insights reveals a previously unexplored molecular architecture, providing a foundation for the rational design of multifunctional optical switching materials.

2. Material and methods

2.1. Material

3-Amino-1,2,4-triazole was purchased from Alfa Aesar Company based in Haverhill, MA, USA. **1E** (1R = 2R = 3R = Me and X = O), **2E** (1R = Me; (2R)(3R)C = Adamantylidene, and X = O), and **3E** (1R = 2R = 3R = Me and X = S) were synthesized through a multistep reaction as reported in the literature [38].

2.2. Methods

The ^{1}H NMR spectra were obtained using an Agilent 600 MHz NMR spectrometer. The mass spectra of compounds **4E**, **5E**, and **6E** were obtained using high-performance liquid chromatography coupled with high-resolution time-of-flight mass spectrometry (LC-MS/QTOF). FT-IR spectra were obtained using a PerkinElmer Spectrum 100 FT-IR Spectrometer (PerkinElmer, Inc., Waltham, MA, USA).

Fluorescence spectra were obtained using an Agilent Cary Eclipse Fluorescence Spectrophotometer (Agilent Technologies, Inc., Santa Clara, CA, USA). UV-Vis spectra were obtained using an Agilent Cary 60 UV-Vis Spectrophotometer (Agilent Technologies, Inc.). UV light irradiation at 366 nm was conducted using an 8W Three-Way UV lamp from Cole-Parmer Instruments Co., Vernon Hills, IL, USA. Irradiation using visible light at 530 nm was performed with an Obelux Lights Green (Obelux Oy, Helsinki, Finland). A Büchi Melting Point B-540 was used to determine melting points. Toluene was dehydrated using sodium wire. Silica gel 60 (0.063–0.200 mm) was utilized for column chromatographic separation, using a mixture of ethyl acetate and hexane as the eluent. An analytical thin layer chromatography (TLC) was performed utilizing Merck precoated silica gel 60 GF-254 plates with a thickness of 250 μm.

2.3. Synthesis

2.3.1. (E)-3-(1-(2,5-dimethylfuran-3-yl)ethylidene)-1-(1H-1,2,4-triazol-3-yl)-4-(propan-2-ylidene)pyrrolidine-2,5-dione (4E)

(1E)-Fulgide (0.115 g, 0.443 mmol) and 1H-1,2,4-triazol-3-amine (0.048 g, 0.576 mmol) were subjected to reflux in dry toluene (20 mL) using a Dean-Stark apparatus for approximately 70 h. The reaction was carried out in an argon atmosphere and in the absence of light. The reaction vessel was periodically monitored using thin-layer chromatography (TLC). The solvent was subsequently removed under vacuum. The mixture was purified using column chromatography with a silica gel and ethyl acetate/n-hexane combination, resulting in an orange solid product weighing 0.025 g and a yield of 17%. Melting Point (Mp): 121-126 °C. 1H NMR (600 MHz, $CDCl_3$, parts per million, Fig. S1) δ_H: 13.21 (1H, s, triazole-NH), 8.31 (1H, s, triazole-H), 5.93 (1H, s, furyl-H), 2.61 (3H, s, Me), 2.36 (3H, s, Me), 2.25 (3H, s, Me), 2.04 (3H, s, Me), 1.38 (3H, s, Me). Calculated for $C_{17}H_{18}N_4O_3$: 326.35; ESI-MS: 326.812 (M^+). FT-IR (ATR, neat) $\tilde{\nu}/cm^{-1}$: 3070, 2923, 2851, 1747, 1724, 1694, 1609, 1570, 1491, 1440.

2.3.2. (E)-3-(adamantylidene)-4-(1-(2,5-dimethylfuran-3-yl) ethylidene)-1-(1H-1,2,4-triazol-3-yl)pyrrolidine-2,5-dione (5E)

(2E)-Fulgide (0.156 g, 0.443 mmol) and 1H-1,2,4-triazol-3-amine (0.048 g, 0.576 mmol) were subjected to reflux in dry toluene (20 mL) using a Dean-Stark apparatus for approximately 70 h. The reaction was carried out in an argon atmosphere and in the absence of light. The reaction vessel was periodically monitored using thin-layer chromatography (TLC). The solvent was subsequently removed under vacuum. The mixture was purified using column chromatography with a silica gel and ethyl acetate/n-hexane combination, resulting in a yellow solid product weighing 0.061 g and a yield of 33%. Melting Point (Mp): 210-215 °C. 1H NMR (300 MHz, CDCl3, parts per million, Fig. S2) δ_H: 12.66 (1H, s, triazole-NH), 8.27 (1H, s, triazole-H), 5.94 (1H, s, furyl-H), 4.42 (1H, broad s, adamantyl-H), 2.54 (3H, s, Me), 2.42 (1H, broad s, adamantyl-H), 2.25 (3H, s, Me), 2.07 (3H, s, Me), 1.95-1.60 (12H, m, adamantyl-H). The molecular weight for $C_{24}H_{26}N_4O_3$ was calculated to be 418.49, with an ESI-MS measurement of 418.816 (M^+). FT-IR (ATR, neat) $\tilde{\nu}/cm^{-1}$: 3077, 2906, 2846, 1736, 1694, 1614, 1572, 1490, 1443.

2.3.3. (E)-3-(1-(2,5-dimethylthiophen-3-yl) ethylidene)-4-(propan-2-ylidene)-1-(1H-1,2,4-triazol-3-yl) pyrrolidine-2,5-dione (6E)

(3E)-Fulgide (0.12 g, 0.434 mmol) and 1H-1,2,4-triazol-3-amine (0.047 g, 0.565 mmol) were subjected to reflux in dry toluene (20 mL) using a Dean-Stark apparatus for approximately 70 h. The reaction was carried out in an argon atmosphere and in the absence of light. The reaction vessel was periodically monitored using thin-layer chromatography (TLC). The solvent was subsequently removed under vacuum. The mixture was purified using column chromatography with a silica gel and ethyl acetate/n-hexane combination, resulting in a pink solid product weighing 0.071 g and a yield of 47%. Melting Point

(Mp): 127-132 °C. 1H NMR (300 MHz, $CDCl_3$, parts per million, Fig. S3) δ_H: 12.70 (1H, s, triazole-NH), 8.29 (1H, s, triazole-H), 6.53 (1H, s, thienyl-H), 2.63 (3H, s, Me), 2.39 (3H, s, Me), 2.32 (3H, s, Me), 2.17 (3H, s, Me), 1.29 (3H, s, Me). For the compound $C_{17}H_{18}N_4O_2S$, the calculated molecular weight is 342.42; ESI-MS analysis indicates a mass of 342.020 (M^+). FT-IR (ATR, neat) $\tilde{\nu}/cm^{-1}$: 2937, 1754, 1731, 1699, 1628, 1570, 1489, 1439, 1369.

2.4. Computational methods

The initial 3D molecular geometries of triazole-fulgimides were constructed and pre-optimized using the MMFF94 force field as implemented in Avogadro [39], followed by full geometry optimization using density functional theory (DFT) with Becke's three parameters gradient-corrected exchange functional and Lee-Yang-Parr gradient-corrected correlation functional (B3LYP) along with a 6-31 + G(d,p) basis set. Harmonic vibrational frequency calculations at the same level of theory confirmed that all optimized structures correspond to true minima on the potential energy surface, as indicated by the absence of imaginary frequencies. Frontier molecular orbitals and the corresponding energy gaps (ΔE) were obtained from the optimized geometries to support analysis of the photochromic ring-opening and ring-closing processes.

Vertical excitation energies and absorption spectra were calculated using time-dependent density functional theory (TD-DFT) with both the B3LYP and the Coulomb-attenuating method combined with B3LYP (CAM-B3LYP) functional, employing the same basis set as used for ground-state geometry optimization. Benchmark calculations performed for the **4E** isomer showed that CAM-B3LYP reproduced the experimental absorption maximum with good accuracy (λ_{cal} = 253 nm versus λ_{exp} = 252 nm), whereas the conventional B3LYP functional significantly overestimated the excitation wavelength (λ_{cal} = 313 nm). Based on this comparison, the CAM-B3LYP level of theory was selected for calculating the excited-state properties of all remaining systems. Solvent effects were included using the conductor-like polarizable continuum model (CPCM), with toluene chosen to replicate the experimental conditions. All calculations were carried out using Gaussian 16 [40].

3. Results and discussion

This study presents the synthesis of three (3) new 1,2,4-triazole-linked fulgimides (**4E, 5E,** and **6E)** through the prolonged reflux of previously synthesized photochromic fulgides **1E, 2E,** and **3E** with 3-amino-1,2,4-triazole in toluene, using a Dean-Stark apparatus under an inert atmosphere with product yields of 17%, 33% and 47%, for 4E, 5E and 6E, respectively (Fig. 1). The modest yields, most notably that of 4E, are likely due to the extreme sensitivity of the precursors to environmental conditions, including light, temperature, and solvent purity. Yield fluctuations similar to those observed here have been reported in previous studies [41,42]. For instance, insufficiently dried solvents can induce hydrolytic cleavage of the fulgide moiety, thereby preventing condensation with the amine and reducing the yield of the target fulgimide. The newly synthesized photochromic compounds were characterized using spectroscopic techniques, including ^{1}H NMR, mass spectrometry, and FT-IR, as well as by their photochromic characteristics. In the ^{1}H NMR analyses of the new fulgimides, minor isomeric structures were observed, particularly noticeable isomerization in **4E**. The structural isomerization observed in the triazole-fulgimides is assumed to result from prolonged reflux with the polar protic 3-amino-1,2,4-triazole. The clean mass spectra of these compounds, indicate that the observed impurities are likely due to isomerization as revealed by ^{1}H NMR spectra.

3.1. Photochromic properties

The ring-closure and ring-opening photoreactions of triazole-fulgimides (**4E**, **5E** and **6E**) in toluene were conducted using UV light at 366 nm and visible light at 530 nm, respectively. Similar to other fulgimides, the triazole-fulgimides were found to convert to their C-forms (**4C**, **5C** and **6C**), which possess high conjugation, when exposed to UV light in toluene. The photoreaction resulted in the transformation of colorless or nearly colorless solutions into colored solutions. The colored solutions in the photostationary state (PSS), containing the C-forms, underwent a ring-opening photoreaction with visible light (530 nm), resulting in the conversion of fulgimides to their colorless E-forms. Fig. 2 illustrates the structural transformations

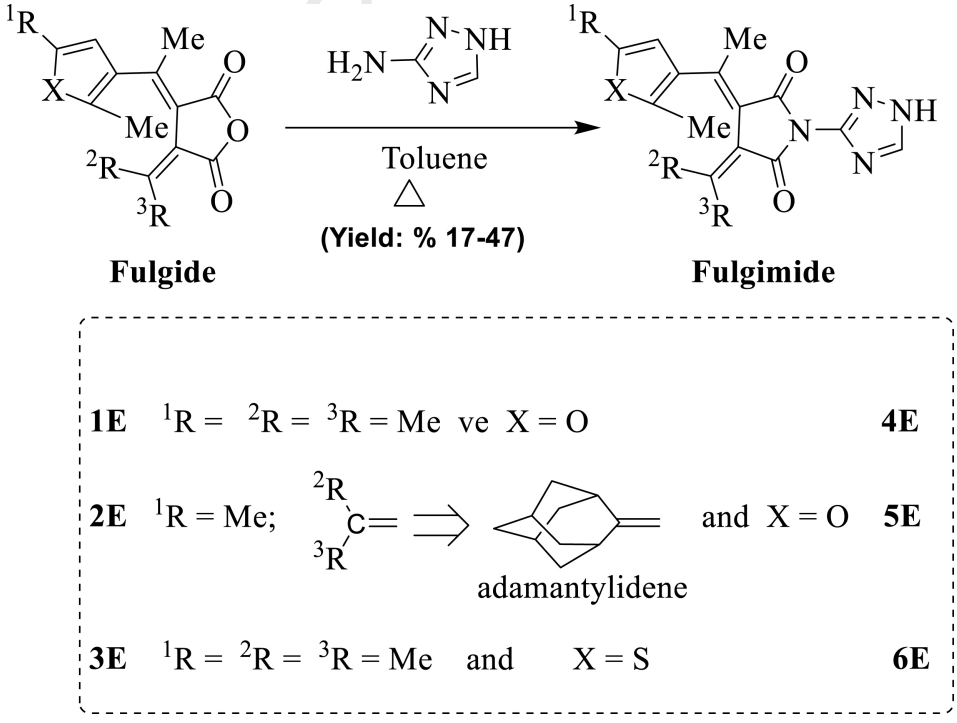

Fig. 1. Synthesis of fulgimides.

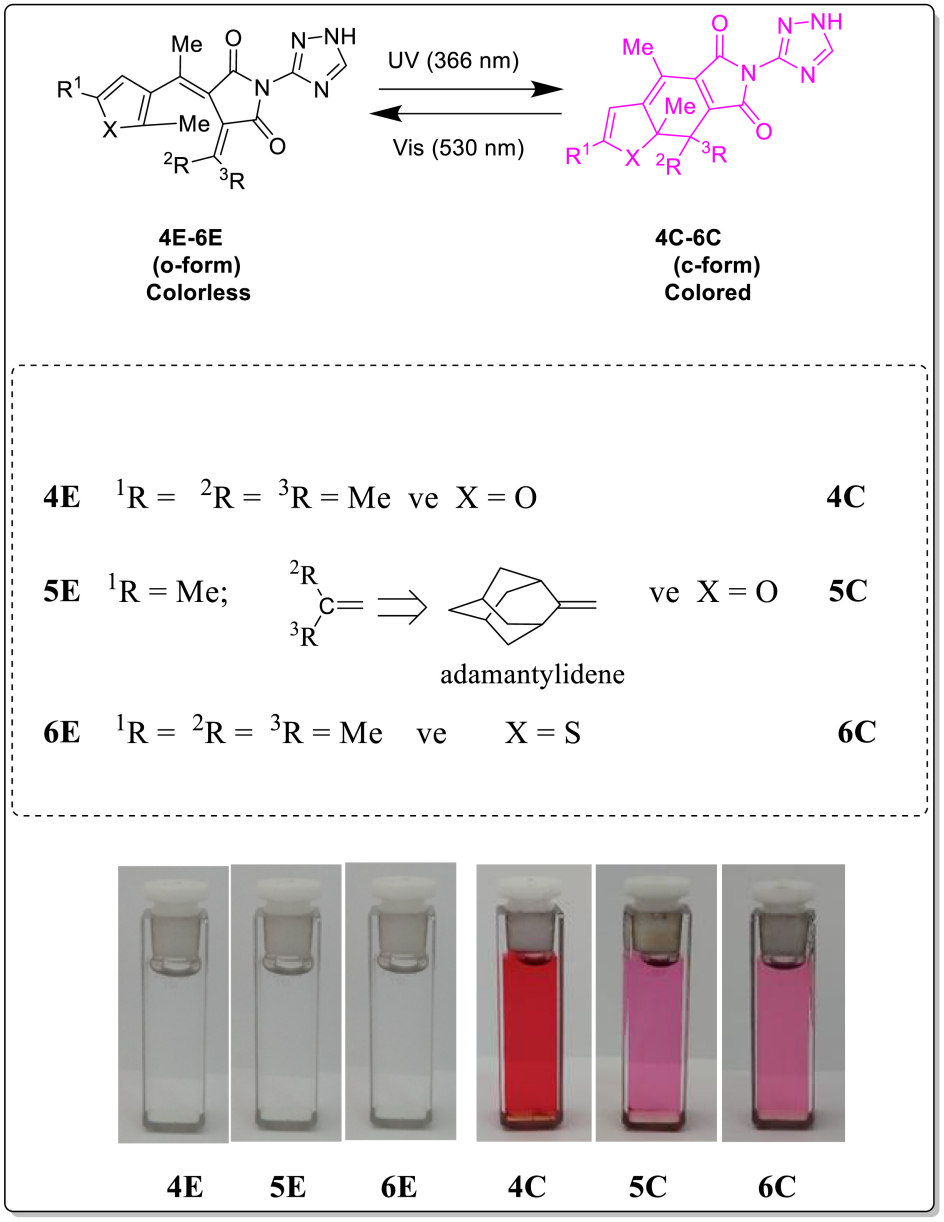

Fig. 2. Photoreactions of triazole-fulgimides in toluene and the observed color changes. (For interpretation of the references to color in this figure legend, the reader is referred to the Web version of this article.)

and the corresponding color changes observed during the bulk ring-closing (forward) and ring-opening (reverse) photoreactions of triazole-fulgimides.

For example, Fig. 3 shows the detailed changes in the UV-Vis absorption spectra of fulgimide **4E** in toluene prior to and during the photoreaction. In toluene (1×10^{-4} M), fulgimide **4E** exhibits UV absorption below 400 nm, with a maximum at 252 nm, corresponding to an initially colorless solution. Fig. 3 (a) presents the UV-Vis spectral bands indicating the conversion of **4E** (E-form) to its C-form upon exposure to UV light at 366 nm. The photoreaction process of the colorless solution transformed to dark red, achieving its photostationary state (PSS) within 7 min under the specified conditions. The C-form (**4C**) at the PSS exhibited an absorption band (λ_{max}) at 505 nm.

Fig. 3 (b) presents the UV-Vis spectra obtained during the reverse photoreaction from **4C** (at PSS) to **4E**. Exposure of the colored solution containing **4C** at PSS to 530 nm light for specific time intervals resulted in a gradual fading of the red color. After approximately 30 min, the initial colorless solution was restored as **4C** converted back to **4E.** Similarly, the forward and reverse photoreactions of **5E** and **6E** in toluene were conducted, with the UV-Vis spectral changes before and after the photoreactions as presented in the supporting information (Figs. S7 and S8). The UV-Vis spectral data for the triazole-fulgimides (**4E, 5E, 6E)** prior to and during the photoreaction are presented in Table 1.

Table 1 shows that the transformation of triazole-fulgimides from their E-forms to C-forms in toluene produced a bathochromic shift of approximately 250 nm. For instance: **4E** (λ_{max} = 252 nm) transitions to **4C** (λ_{max} = 505 nm). This tendency was similarly observed in the previous studies [9,25,28] where E-forms of photochromic compounds were converted to C-forms.

The ring-closed forms (C-forms) of triazole-fulgimides were also compared with the ring-closed forms (C-forms) of the original fulgides. The transformation of fulgides into their respective triazole-fulgimides did not only affect the thermal stabilities [9] but also resulted in a minimal bathochromic shift in the absorption maximum wavelengths (λ_{max}) of the ring-closed forms. The ring-closed forms of the respective fulgides and fulgimides in toluene were observed as follows: **1C** (λ_{max} = 495 nm)

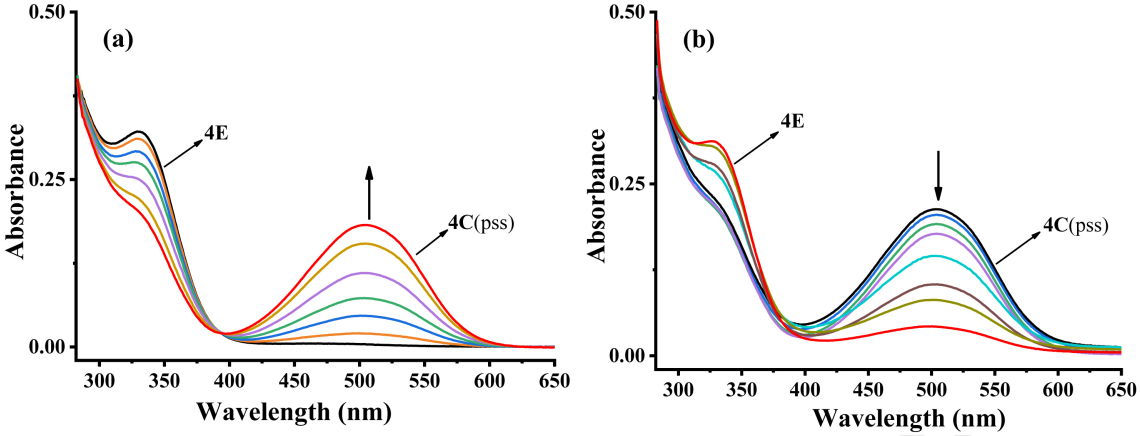

Fig. 3. Observed changes in the absorption spectra of fulgimide **4E** in toluene (1×10^{-4} M): (a) Conversion from **4E** to **4C** (PSS) (λ = 366 nm) (0 s, 10 s, 30 s, 1 min, 2 min, 4 min, and 7 min (PSS)); (b) Conversion from **4C** (PSS) back to **4E** (λ = 530 nm) (0 s, 30 s, 1 min, 2 min, 7 min, 12 min, 18 min, 30 min).

Table 1
Absorption data (UV-Vis) of the triazole-fulgimides in Toluene.

Compounds	Experimental absorption data	Calculated absorption data	Quantum Yields data
	$\lambda_{max}/(\varepsilon_{max}) \rightarrow \lambda_{max}$ (A)[a]	$\lambda_{max}/(\varepsilon_{max}) \rightarrow \lambda_{max}$ (f)	$\Phi_{E\rightarrow C}/\Phi_{C\rightarrow E}$
4E→4C	252/(10308)→505 (0.21)	253 (13000) →500 (0.24)	0.69/0.01
5E→5C	276/(13310)→529 (0.12)	274 (14000) →512 (0.20)	0.32/0.18
6E→6C	277 (10188)→527 (0.19)	266 (10000) →505 (0.24)	0.26/0.03

1) Cell length: 1 cm. Concentration: 1.0×10^{-4} M.
[a] λ_{max}/nm (ε_{max}/mol^{-1} dm^3 cm^{-1}) → λ_{max}/nm (absorbance).

to **4C** (λ_{max} = 505 nm); **2C** (λ_{max} = 511 nm) to **5C** (λ_{max} = 529 nm); and **3C** (λ_{max} = 524 nm) to **6C** (λ_{max} = 527 nm). Similar comparisons have been made in the previous studies, where fulgimides were observed to absorb at longer wavelengths compared to their original fulgides [23]. However, when the absorption intensities of the fulgides are compared with those of their corresponding fulgimides, a significant decrease in the absorption intensity of the fulgimides was observed (Hypochromic Effect). Fig. 4 shows a comparison of the UV-Vis absorption spectra of the fulgides **1C, 2C,** and **3C** with their corresponding triazole-fulgimides, **4C, 5C,** and **6C**, respectively.

Quantum yields of ring closure ($\Phi_{E\rightarrow C}$) for the 4E, 5E and 6E, and the ring opening quantum yields ($\Phi_{C\rightarrow E}$) for the colored forms 4C, 5C and 6C were measured using a chemical actinometer, Aberchrome 540, as described by Heller et al. 12 [38]. Quantum yields are given in Table 1. When the ring-closing (ΦE→C) and ring-opening (ΦC→E) quantum yields of synthesized photochromic fulgimide derivatives were examined, it was observed that the heteroaromatic ring structure and steric effects play a decisive role in the quantum yields. The furan derivatives 4E (0.69) and 5E (0.32) exhibited higher ring-closing quantum yields compared to the thiophene derivative 6E (0.26); this was attributed to the lower aromatic stabilization energy of the furan ring relative to thiophene. The higher aromatic stability of the thiophene ring creates resistance to the ring-closing process, leading to a lower conversion yield in compound 6E. On the other hand, when comparing the furan derivatives among themselves, the observed decrease in yield for compound 5E can be explained by the steric hindrance caused by the incorporated adamantyl group, which prevents the molecule from adopting the favorable conformation required for ring closure. In contrast, the highest ring-opening quantum yield was observed for compound 5E, which possesses the bulky adamantyl group. Consistent with the literature, this arises because bulky substituents such as adamantylidene introduce structural strain on the closed form, increasing the system's tendency to return to the ground state and thereby significantly enhancing the ring-opening quantum yield [7,43].

3.2. Computational results

Geometry optimizations were performed to analyze the ground state electronic structures of compounds **4E-6E** in their open and closed ring forms. The optimized geometries provide a structural basis for interpreting the experimentally observed photochromic behavior, as variations in molecular conformation and π-conjugation directly affect electronic delocalization, frontier orbital energies, and optical response. Therefore, the theoretical calculations complement the experimental results by providing molecular level insight into the ring-opening and ring-

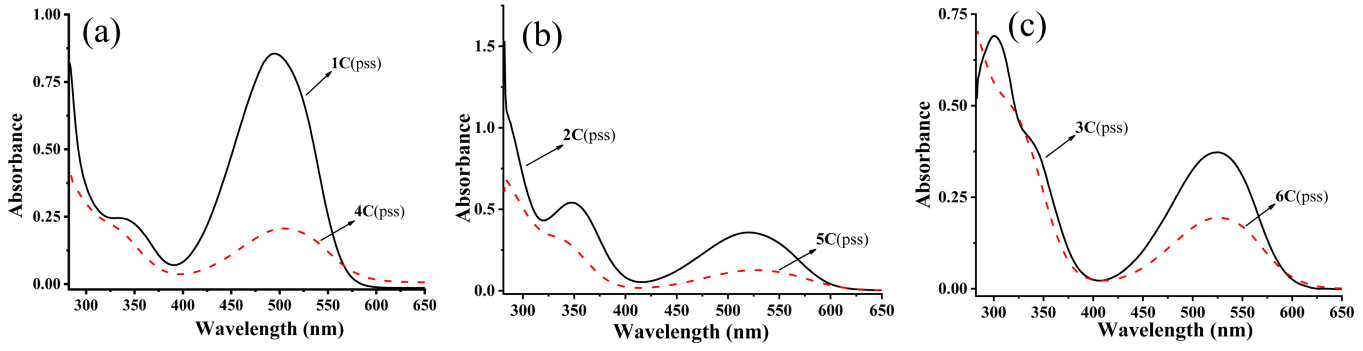

Fig. 4. Comparison of the C-form of the fulgides with the corresponding C-form of the triazole-fulgimides (in toluene, 1×10^{-4} M, at the photostationary state).

closing processes underlying the observed spectral changes. The optimized structures were used for subsequent frontier molecular orbital and absorption spectra analyses are provided in the Supporting Information (Fig. S9).

3.3. Frontier orbitals and photochromic switching

Fig. 5 shows the frontier molecular orbitals (FMOs) and HOMO-LUMO energy gaps (ΔE) for the open (o-form) and closed (c-form) isomers of compounds **4E-6E**. Distinct electronic signatures between the two photochromic states rationalize their light-induced ring-opening and ring-closing behavior. In all closed forms (**4C–6C**), the HOMO is extensively delocalized over the cyclic π-framework, while the LUMO displays significant density along the photoactive bond region. Photoexcitation therefore, promotes HOMO→LUMO transitions with pronounced antibonding character at the cyclized moiety, facilitating light-induced ring opening. In contrast, the open forms (**4E–6E**) exhibit more localized frontier orbitals with reduced conjugation, consistent with their higher-energy absorption and enhanced flexibility required for photocyclization. Ring closure leads to pronounced HOMO–LUMO gap narrowing, reflecting increased π-delocalization and explaining the experimentally observed bathochromic shift in the UV-Vis spectra of the closed isomers. The calculated ΔE decreases from 4.12 to 2.69 eV for compound **4E**, from 4.15 to 2.65 eV for compound **5E**, and from 4.21 to 2.57 eV for compound **6E**. These trends directly correlate with red-shifted absorption and stronger visible-light responsiveness upon cyclization.

Among the series, compound **6E** exhibits the most favorable electronic features. Its closed form (**6C**) possesses the smallest ΔE and the most delocalized HOMO-LUMO pair, indicating superior electronic coupling through the π-system and intensified low-energy absorption. Moreover, the LUMO of **6C** is optimally aligned along the photoactive bond, maximizing antibonding character and promoting photoinduced ring opening. Although the open form (**6E**) retains a larger ΔE, sufficient orbital overlap and redistribution enable effective ring closure, ensuring reversibility. Comparatively, the photochromic performance follows the order **6E** > **5E** ≈ **4E**, consistent with the magnitude of ΔE modulation and empirical observations in UV–Vis absorption shifts, identifying compound **6E** as the most promising photochromic candidate in this series.

3.4. Absorption spectra and photochromism

The TD-DFT simulated absorption spectra of compounds **4E–6E** in their open (E) and closed (C) forms are shown in Fig. 6, and the absorption properties are presented in Table 1. The spectra reflect the electronic trends discussed in FMOs and exhibit the characteristic optical response of photochromic systems. In all cases, a clear spectral contrast is observed between the two isomeric states, with the appearance of a new low-energy absorption band upon ring closure. The open ring isomers (**4E**, **5E** and **6E**) display intense absorption bands in the 200–330 nm region, originating predominantly from localized π→π* transitions, with negligible absorption in the visible region. This behavior indicates that the open forms are optically transparent under visible light, enabling high switching contrast.

In contrast, the closed isomers (**4C–6C**) display an additional broad absorption band in the visible region (~480–560 nm), which is absent in the open forms. This low-energy band is primarily associated with HOMO→LUMO excitations involving delocalized frontier orbitals across the cyclized π-framework. The pronounced bathochromic shift upon ring closure is consistent with the reduced HOMO–LUMO gaps and increased conjugation, and it provides the optical basis for the colored photochromic state observed experimentally. Additionally, the comparative analysis shows that compound **6E** exhibits the strongest optical response, combining intense UV absorption in the open form with a well-defined and strongly absorbing visible band in the closed form. The combined spectra further reveal minimal spectral overlap between open

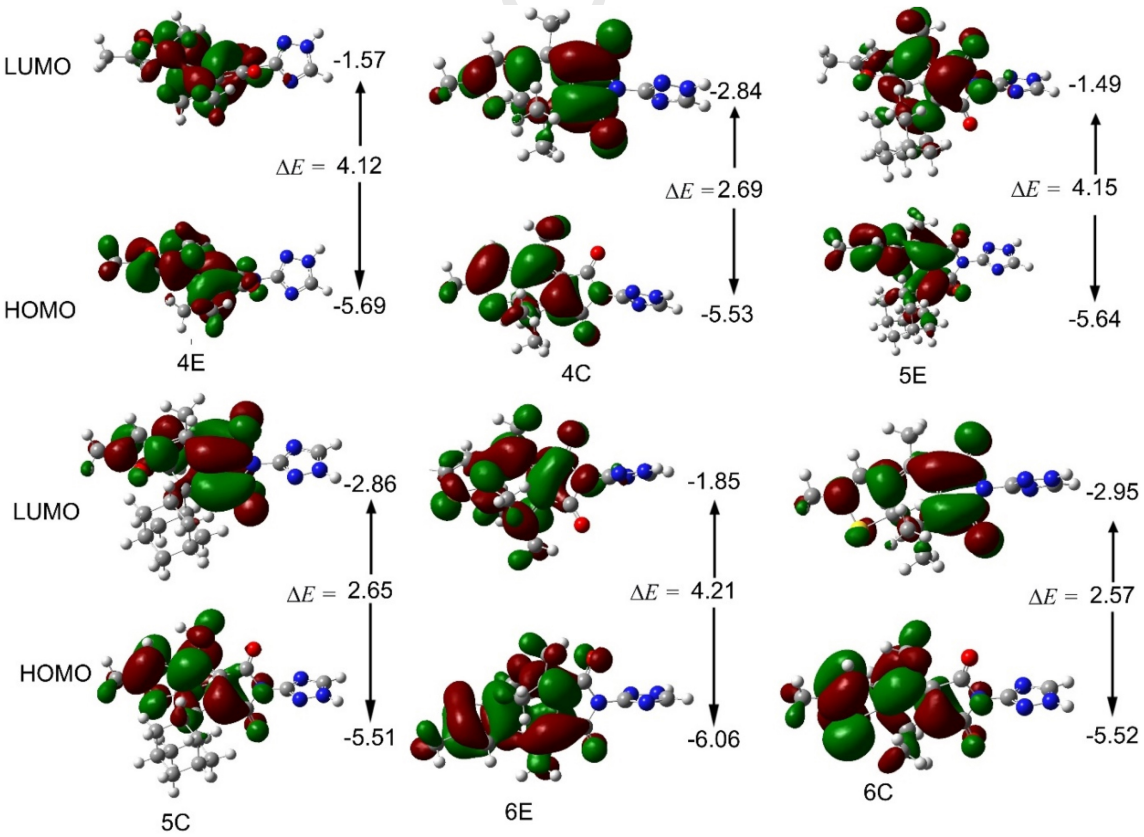

Fig. 5. Frontier molecular orbitals and corresponding HOMO–LUMO energy gaps (ΔE, eV) of compounds **4E–6E** in their open (E) and closed (C) photochromic forms.

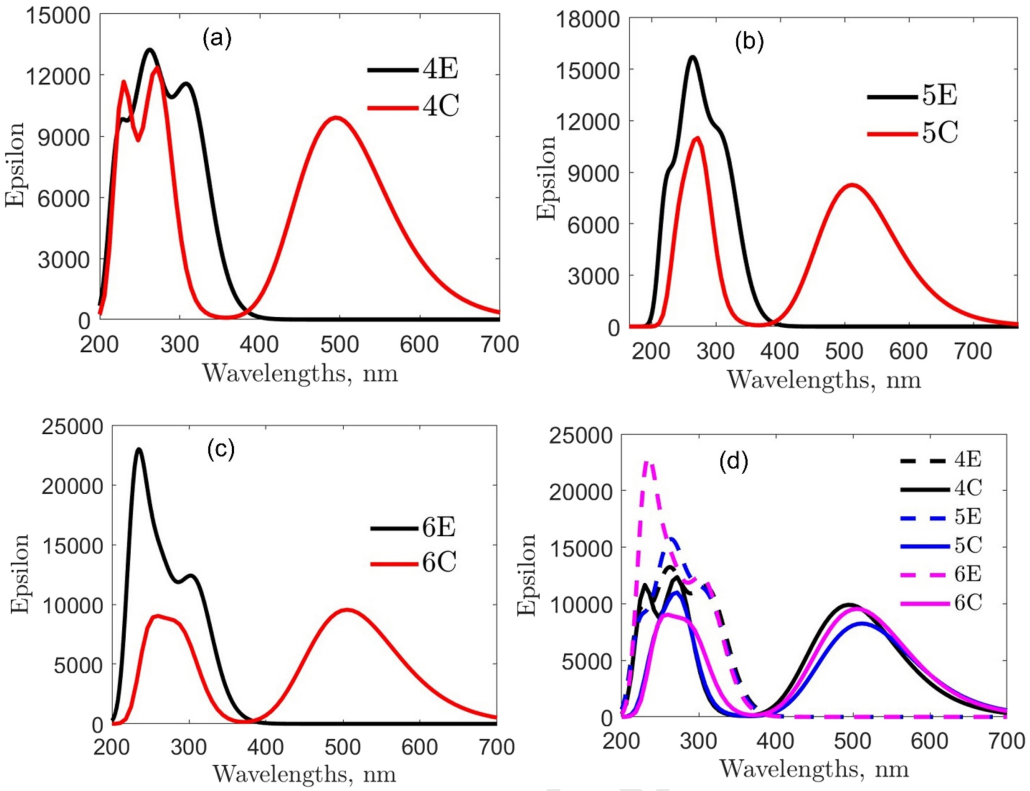

Fig. 6. The TD-DFT/CAM-B3LYP/6-31 + *G*(d,p) computed absorption spectra of the open (E) and closed (C) photochromic forms of compounds **4E-6E:** (a) **4E**/**4C**, (b) **5E**/**5C**, (c) **6E**/**6C**, and (d) combined spectra for all compounds.

and closed isomers above ~450 nm, enabling selective optical addressing and efficient switching. Consistent with the frontier orbital analysis, the overall photochromic performance inferred from the absorption behavior follows the trend **6E** > **5E** ≈ **4E**, identifying compound **6E** as the most promising photochromic candidate in this series.

3.5. *Fluorescent properties of triazole fulgimides*

The fluorescent properties of triazole fulgimides (**4E**, **5E**, and **6E**) were examined in toluene at ambient temperature. Upon excitation with 300 nm light (λex = 300 nm), toluene solutions of the triazole fulgimides **4E**, **5E**, and **6E** displayed emission bands at approximately 504 nm, 530 nm, and 529 nm, respectively. The observed fluorescent properties in the synthesized triazole fulgimides can be explained as follows: The 1,2,4-triazole ring, linked to the fulgimide at the 3-position, features an N-H hydrogen on the nitrogen at position 1. The N-H hydrogen at position 1 is assumed to undergo tautomerization, potentially isomerizing to form a hydrogen bond with the imide carbonyl group (Fig. 7). Consequently, the presence of the hydrogen bond indicates that the triazole ring and the imide ring are coplanar, facilitating conjugation between the triazole and imide rings. The triazole fulgimides likely acquired their fluorescent properties as a result.

The fluorescent behavior of the ring-closed forms of triazole-linked fulgimides was examined by exposing the respective fulgimides in toluene to UV light until reaching the photostationary state (PSS), after which their fluorescence spectra were measured again. Fig. 8 shows the changes in the fluorescence emission spectra of triazole fulgimides before and after photoreaction with 366 nm UV light at their photostationary state (PSS).

A marked fluorescence quenching is observed for the PSS C-forms, yielding intensity reductions of 20% (5E), 30% (4E), and 40% (6E). Although not directly applicable in their present form, these quenching efficiencies represent a highly promising starting point. Through structural modification such as the systematic replacement of key sub-

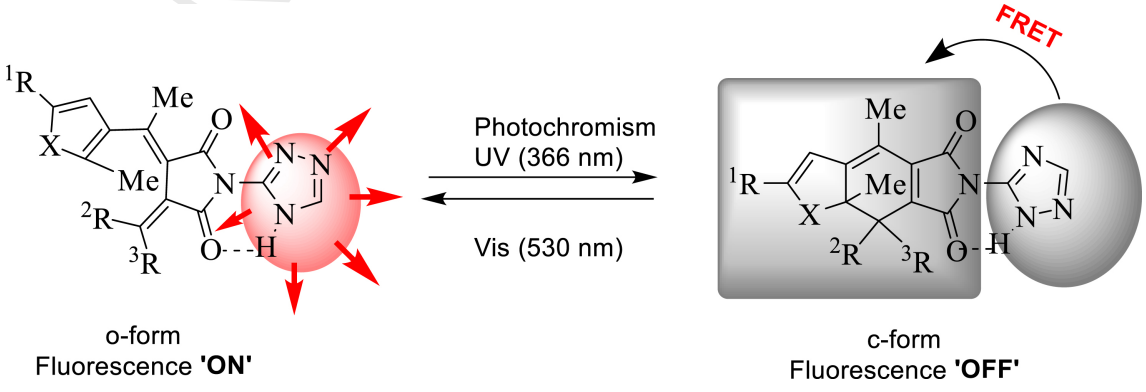

Fig. 7. The FRET observed in the ring-closed forms of the triazole-fulgimides.

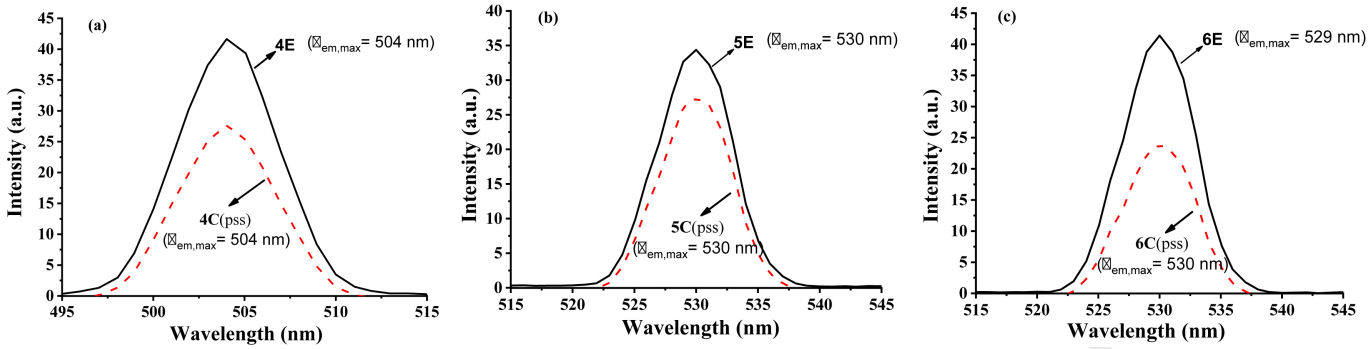

Fig. 8. Changes observed in the fluorescence emission spectra of triazole fulgimides **4E, 5E, and 6E** before and after photoreaction with 366 nm UV light (**4C, 5C, and 6C** at PSS, respectively) (in toluene, 1×10^{-4} M; λex = 300 nm).

stituents on the fluorophore or switching core, it is possible to elevate performance. Through this paradigm, these compounds could be tuned into a promising candidate for applications including optical memory and super-resolution imaging. Table 2 presents the relative comparative values for the fluorescence intensities of the E– and C-forms.

With only a few exceptions [44], an open ring form of fluorescence-switchable fulgide derivative displays an intense fluorescence emission band in the visible region, while the fluorescence of its C-form solution is quenched significantly [42,45,46]. The fluorescence quenching observed in the ring-closed forms (C-forms) of triazole-fulgimides may be attributed to FRET from the fluorescent triazole ring to the conjugated fulgimide structure in the C-form. The fluorescence quantum yields of all synthesized fulgimide derivatives were measured using anthracene as a reference material. For all three compounds, the fluorescence quantum yields Q_f for 4E, 5E and 6E for ring-closing were found to be 5.1×10^{-4}, 8.3×10^{-4} and 6.2×10^{-4} respectively.

It is widely accepted in the literature that fulgide and fulgimide derivatives generally do not exhibit emission at room temperature unless they structurally contain a fluorescent group. In our study, the fluorescence quantum yields of the synthesized derivatives (4E–6E) were obtained in the range of 5.1×10^{-4} to 8.3×10^{-4}, which are consistent with the findings reported in the literature. Notably, a significant decrease in fluorescence quantum yield values was observed upon transitioning from the open (E) form to the closed (C) form. This decrease can be explained by the lower excited-state energy level of the C-form compared to the E-form, causing the C-form to act as an energy trap [7]. Consequently, the excited-state energy is primarily channeled into the electrocyclic ring-closure reaction rather than fluorescence emission, or it is quenched through non-radiative pathways.

4. Conclusion

This work demonstrates a structure-encoded strategy for coupling photochromism and fluorescence switching within a single organic photo-switch by covalently embedding a 1,2,4-triazole unit into the imide framework of fulgimides. The resulting materials display photochromism based on the interconversion between open and closed forms, large visible-range spectral contrast, and reversible fluorescence modulation under alternating UV and visible light. Experimentally observed fluorescence quenching in the closed form is governed by efficient intramolecular energy transfer, while quantum-chemical analysis reveals that photoinduced cyclization drives substantial π-delocalization and HOMO-LUMO gap compression, directly controlling the optical response. The strong agreement between experiment and theory establishes clear, predictive structure-property relationships and identifies heteroatom-assisted imide functionalization as a powerful design lever. By unifying photostability, fluorescence tunability, and electronic predictability, this platform advances organic photo-switches toward practical light-regulated materials for optical memory, sensing, and adaptive photonic systems.

Table 2
Fluorescence emission data of the triazole-fulgimides in toluene.

Compounds	Solution	λem/nm (rel. int) → λem/nm (rel. int)
4E → 4C	Toluene	504 (1) →504 (0.7)
5E →5C	Toluene	530 (1) → 530 (0.8)
6E → 6C	Toluene	529 (1) →529 (0.6)

Concentration: 1×10^{-4} M; Excitation wavelength: λ_{ex} = 300 nm.

CRediT authorship contribution statement

Khamis Nassor Ally: Conceptualization, Data curation, Formal analysis, Investigation, Methodology, Visualization, Writing – original draft. **Melkizedeck Hiiti Tsere:** Data curation, Formal analysis, Methodology, Software, Visualization, Writing – original draft. **Said Ali Vuai:** Supervision, Validation, Writing – review & editing. **Azaria Stephano Lameck:** Data curation, Formal analysis, Visualization, Writing – original draft. **Leyla Öztürk:** Conceptualization, Data curation, Formal analysis, Investigation, Methodology, Writing – review & editing. **Mahmut Köse:** Conceptualization, Project administration, Supervision, Validation, Visualization, Writing – review & editing.

Declaration of competing interest

The authors declare that they have no known competing financial interests or personal relationships that could have appeared to influence the work reported in this paper.

Acknowledgment

The authors gratefully acknowledge the financial support provided by Zonguldak Bülent Ecevit University, Scientific Researches Department (Project number: 2018-72118496-01).

Appendix A. Supplementary data

Supplementary data to this article can be found online at https://doi.org/10.1016/j.jlumin.2026.121963.

Data availability

Data will be made available on request.

References

[1] L. Mao, H. Ding, X. Li, G. Liu, S. Pu, A diarylethene-based fluorescent chemosensor for highly selective recognition of Zn2+ and its application, J. Photochem. Photobiol. Chem. 431 (2022) 114011, https://doi.org/10.1016/j.jphotochem.2022.114011.

[2] W. Wang, Y. Cheng, X. Xie, Design and applications of photochromic compounds for quantitative chemical analysis and sensing, Chem. Commun. 61 (46) (2025) 8327–8338, https://doi.org/10.1039/D5CC01830G.

[3] H. Pacheco Hernandez, S. Hecht, W. Wenzel, L. Heinke, M. Kozlowska, Photoswitching conduction in framework materials, Adv. Funct. Mater. (2025) e12262, https://doi.org/10.1002/adfm.202512262. *n/a*(n/a).

[4] S. Mitra, M. Zhang, S.F. Bittmann, J. Cai, X. Dong, R.S. Murphy, …R.D. Miller, Elucidating the reaction kernel and probing the effect of anharmonicity in the ring-closing reaction of fulgide single crystals, JCS (J. Chromatogr. Sci.) 16 (41) (2025) 19118–19129, https://doi.org/10.1039/D5SC03764F.

[5] H. Bouas-Laurent, H.J.P. Dürr, A. Chemistry, Organic Photochromism (IUPAC Technical Report), vol. 73, 2001, pp. 639–665, https://doi.org/10.1351/pac200173040639, 4.

[6] Z. Li, J. Song, Q. Wang, Y. Qi, X. Gao, Y. Feng, …J. Yin, Near-infrared light-activated switchable antibacterial agent based on dithienylethene photoswitch, Chin. Chem. Lett. 37 (4) (2026) 111139, https://doi.org/10.1016/j.cclet.2025.111139.

[7] Y. Yokoyama, Fulgides for memories and switches, Chem. Rev. 100 (5) (2000) 1717–1740, https://doi.org/10.1021/cr980070c.

[8] F. Renth, F. Temps, Fulgides and fulgimides, in: Molecular Photoswitches, 2022, pp. 177–192.

[9] J. Zhang, H. Tian, The endeavor of diarylethenes: new structures, high performance, and bright future, Adv. Opt. Mater. 6 (6) (2018) 1701278, https://doi.org/10.1002/adom.201701278.

[10] A.G. Lvov, Y. Yokoyama, V.Z. Shirinian, Post-modification of the ethene bridge in the rational design of photochromic diarylethenes, Chem. Rec. 20 (1) (2020) 51–63, https://doi.org/10.1002/tcr.201900015.

[11] D. Lachmann, R. Lahmy, B. König, Fulgimides as light-activated tools in biological investigations, Eur. J. Org Chem. 2019 (31–32) (2019) 5018–5024, https://doi.org/10.1002/ejoc.201900219.

[12] X. Meng, S. Lin, J. Guo, Chiral fluorescent photoswitches: coupling of chirality and fluorescence into photoswitches for photonic applications, Acc. Chem. Res. 58 (16) (2025) 2586–2599, https://doi.org/10.1021/acs.accounts.5c00330.

[13] A.A. Corallo, C. Noli, A. Brizzi, M. Paolino, C. Mugnaini, F. Corelli, Light-controlled modulation of the endocannabinoid system: photoswitchable ligands for cannabinoid and TRPV1 receptors, Int. J. Mol. Sci. 27 (2) (2026) 573, https://doi.org/10.3390/ijms27020573.

[14] Y. Jiao, R. Yang, Y. Luo, L. Liu, B. Xu, W. Tian, Fulgide derivative-based solid-state reversible fluorescent switches for advanced optical memory, CCS Chem. 4 (1) (2021) 132–140, https://doi.org/10.31635/ccschem.021.202000673.

[15] L. Xi, J. Liu, S. Zhang, T. Liu, L. Hou, Combining quantum dots and photochromic molecular switches: next-generation light-responsive materials, Small Methods 9 (8) (2025) 2500192, https://doi.org/10.1002/smtd.202500192.

[16] S. Mollick, J.-C. Tan, Organic solid-state photochromism using porous scaffolds, Nat. Rev. Mater. 10 (7) (2025) 519–535, https://doi.org/10.1038/s41578-024-00760-4.

[17] T. Fukaminato, S. Ishida, R. Métivier, Photochromic fluorophores at the molecular and nanoparticle levels: fundamentals and applications of diarylethenes, NPG Asia Mater. 10 (9) (2018) 859–881, https://doi.org/10.1038/s41427-018-0075-9.

[18] Y. Huang, L. Ning, X. Zhang, Q. Zhou, Q. Gong, Q. Zhang, Stimuli-fluorochromic smart organic materials, Chem. Soc. Rev. 53 (3) (2024) 1090–1166, https://doi.org/10.1039/D2CS00976E.

[19] Z. Li, X. Ma, J. Song, Q. Wang, Y. Feng, H. Liu, …J. Yin, 570 nm/770 nm light-excited deep-red fluorescence switch based on dithienylethene derived from BF2-curcuminoid, Chem. Sci. 16 (4) (2025) 1762–1771, https://doi.org/10.1039/D4SC05473C.

[20] N. Sivasankaran, K. Palaninathan, Photochromic switchable pendant indolyl fulgimide polypyrrole, Polym. Degrad. Stabil. 98 (9) (2013) 1852–1861, https://doi.org/10.1016/j.polymdegradstab.2013.05.009.

[21] M. Bayat, H. Mardani, H. Roghani-Mamaqani, R. Hoogenboom, Self-indicating polymers: a pathway to intelligent materials, Chem. Soc. Rev. 53 (8) (2024) 4045–4085, https://doi.org/10.1039/D3CS00431G.

[22] Z. Li, J.-R. Zhang, X.-K. Tian, S. Yang, S. Chen, H. Zhou, X.-G. Yang, Green-/NIR-light-controlled rapid photochromism featuring reversible thermally activated delayed fluorescence and photoelectronic switching, Chem. Sci. 13 (32) (2022) 9381–9386, https://doi.org/10.1039/D2SC02662G.

[23] Q.-F. Li, L. Zhang, M. Shen, J.-T. Wang, L. Jin, Z. Wang, Photochromic diarylethene induced fluorescence switching materials constructed by non-covalent interactions, J. Mater. Chem. C 11 (38) (2023) 12828–12847, https://doi.org/10.1039/D3TC02310A.

[24] X. Chen, X.-F. Hou, X.-M. Chen, Q. Li, An ultrawide-range photochromic molecular fluorescence emitter, Nat. Commun. 15 (1) (2024) 5401, https://doi.org/10.1038/s41467-024-49670-7.

[25] Z. Zhang, W. Wang, M. O'Hagan, J. Dai, J. Zhang, H. Tian, Stepping out of the blue: from visible to Near-IR triggered photoswitches, Angew. Chem. Int. Ed. 61 (31) (2022) e202205758, https://doi.org/10.1002/anie.202205758.

[26] J. Du, Z. Yang, H. Lin, D. Poelman, Inorganic photochromic materials: recent advances, mechanism, and emerging applications, Respons. Mater. 2 (2) (2024) e20240004, https://doi.org/10.1002/rpm.20240004.

[27] A. Sharma, R. Dubey, R. Bhupal, P. Patel, S.K. Verma, S. Kaya, V. Asati, An insight on medicinal attributes of 1,2,3- and 1,2,4-triazole derivatives as alpha-amylase and alpha-glucosidase inhibitors, Mol. Divers. 28 (5) (2024) 3605–3634, https://doi.org/10.1007/s11030-023-10728-1.

[28] S.A. Khan, M.J. Akhtar, U. Gogoi, D.U. Meenakshi, A. Das, An overview of 1,2,3-triazole-Containing hybrids and their potential anticholinesterase activities, Pharmaceuticals 16 (2) (2023) 179, https://doi.org/10.3390/ph16020179.

[29] M.J. Vaishnani, S. Bijani, M. Rahamathulla, L. Baldaniya, V. Jain, K.Y. Thajudeen, …I. Pasha, Biological importance and synthesis of 1,2,3-triazole derivatives: a review, Green Chem. Lett. Rev. 17 (1) (2024) 2307989, https://doi.org/10.1080/17518253.2024.2307989.

[30] D.P. Vala, R.M. Vala, H.M. Patel, Versatile synthetic platform for 1,2,3-Triazole chemistry, ACS Omega 7 (42) (2022) 36945–36987, https://doi.org/10.1021/acsomega.2c04883.

[31] D. Lengerli, K. Ibis, Y. Nural, E. Banoglu, The 1,2,3-triazole 'all-in-one' ring system in drug discovery: a good bioisostere, a good pharmacophore, a good linker, and a versatile synthetic tool, Expert Opin. Drug Discov. 17 (11) (2022) 1209–1236, https://doi.org/10.1080/17460441.2022.2129613.

[32] S. Nithyanandan, P. Kannan, K. Senthil Kumar, P. Ramamurthy, Optical switching, photophysical, and electrochemical behaviors of pendant triazole-linked indolylfulgimide polymer, J. Polym. Sci. Polym. Chem. 49 (5) (2011) 1138–1146, https://doi.org/10.1002/pola.24528.

[33] A. Günther, Y. Deja, M. Kilic, K. Tran, P. Kotra, F. Renz, …B. Roth, Investigation of the molecular switching process between spin crossover states of triazole complexes as basis for optical sensing applications, Sci. Rep. 14 (1) (2024) 5897, https://doi.org/10.1038/s41598-024-56427-1.

[34] Y. Tian, S. Zhu, H. Liu, Y. Song, B. Liu, H. Yao, S. Guan, Hyperbranched polyimide with triazole core structure for nonvolatile resistive switching memory, J. Polym. Sci. 62 (10) (2024) 2051–2057, https://doi.org/10.1002/pol.20230909.

[35] A.U. Hassan, S.H. Sumrra, M. Zubair, A. Mohyuddin, G. Mustafa, Design and exploration of benzene like azobis triazoles for long-range push-pull photo-switching attributes, J. Fluoresc. 35 (2) (2025) 731–750, https://doi.org/10.1007/s10895-023-03532-5.

[36] H. Ding, G. Liu, S. Pu, C. Zheng, Multi-addressable fluorescent switch based on a photochromic diarylethene with triazole-bridged methylquinoline group, Dyes Pigments 103 (2014) 82–88, https://doi.org/10.1016/j.dyepig.2013.11.022.

[37] J. Yang, L. Tang, L. Li, X. Wu, L. Yan, Recent advances in organic small-molecule fluorescent probes for the detection of zinc ions ($Zn2+$), J. Fluoresc. 35 (5) (2025) 2641–2674, https://doi.org/10.1007/s10895-024-03770-1.

[38] P.J. Darcy, H.G. Heller, P.J. Strydom, J. Whittall, Photochromic heterocyclic fulgides. Part 2. Electrocyclic reactions of (E)-α-2,5-dimethyl-3-furylethylidene(alkyl-substituted methylene)succinic anhydrides, J. Chem. Soc., Perkin Trans. 1 (1981) 202–205, https://doi.org/10.1039/P19810000202, 0.

[39] M.D. Hanwell, D.E. Curtis, D.C. Lonie, T. Vandermeersch, E. Zurek, G.R. Hutchison, Avogadro: an advanced semantic chemical editor, visualization, and analysis platform, J. J. o. c. (2012).

[40] M. Frisch, G. Trucks, H. Schlegel, G. Scuseria, M. Robb, J. Cheeseman, …H. Nakatsuji, Gaussian 16 Vc. 01 (Revision C. 01), Gaussian, Inc, Wallingford CT, 2019.

[41] E. Orhan, L. Gundogdu, M. Kose, Y. Yokoyama, Synthesis and photochromic properties of 4,5-bisaryl-3(2H)-pyridazinones, J. Photochem. Photobiol. Chem. 314 (2016) 164–170, https://doi.org/10.1016/j.jphotochem.2015.08.025.

[42] K.N. Ally, L. ÖztÜrk, M. KÖse, Photochromic and fluorescence properties of coumarin fulgimides, J. T. J. o. C. 44 (4) (2020) 1031–1042, https://doi.org/10.3906/kim-2003-31.

[43] Y. Yokoyama, T. Goto, T. Inoue, M. Yokoyama, Y.J.C.L. Kurita, Fulgides as Efficient Photochromic Compounds. Role of the Substituent on Furylalkylidene Moiety of Furylfulgides in the Photoreaction, 1988, pp. 1049–1052, 6.

[44] Y. Liang, A.S. Dvornikov, P.M. Rentzepis, Synthesis of novel photochromic fluorescing 2-indolylfulgimides, Tetrahedron Lett. 40 (46) (1999) 8067–8069, https://doi.org/10.1016/S0040-4039(99)01702-5.

[45] J. Walz, K. Ulrich, H. Port, H.C. Wolf, J. Wonner, F. Effenberger, Fulgides as switches for intramolecular energy transfer, Chem. Phys. Lett. 213 (3) (1993) 321–324, https://doi.org/10.1016/0009-2614(93)85139-F.

[46] V.P. Rybalkin, S.Y. Zmeeva, L.L. Popova, K.S. Tikhomirova, Y.V. Revinskii, A.D. Dubonosov, …V.I. Minkin, Photochromic benzo[g]indolyl fulgimide with modulated fluorescence, Russ. J. Org. Chem. 53 (1) (2017) 29–34, https://doi.org/10.1016/0009-2614(93)85139-F.